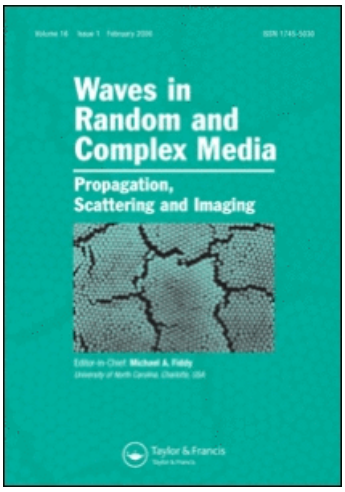

Waves in Random and Complex Media
Publication details, including instructions for authors and subscription information:
http://www.informaworld.com/smpp/title~content=t716100762

Leaky modes in twisted microstructured optical fibers

A. Nicolet [a]; F. Zolla [b]; Y. O. Agha [b]; S. Guenneau [c]
[a] Institut Fresnel, UMR CNRS 6133, Université Paul Cézanne, Marseille, France [b] Institut Fresnel, UMR CNRS 6133, Université de Provence, Marseille, France [c] Institut Fresnel, France

Online Publication Date: 01 November 2007

To cite this Article Nicolet, A., Zolla, F., Agha, Y. O. and Guenneau, S.(2007)'Leaky modes in twisted microstructured optical fibers',Waves in Random and Complex Media,17:4,559 — 570
To link to this Article: DOI: 10.1080/17455030701481849
URL: http://dx.doi.org/10.1080/17455030701481849

Waves in Random and Complex Media
Vol. 17, No. 4, November 2007, 559–570

Leaky modes in twisted microstructured optical fibers

A. NICOLET†*, F. ZOLLA‡, Y. O. AGHA‡ and S. GUENNEAU§

†Institut Fresnel, UMR CNRS 6133, Université Paul Cézanne, Marseille, France
‡Institut Fresnel, UMR CNRS 6133, Université de Provence, Marseille, France
§Institut Fresnel, UMR CNRS 6133, CNRS, France

(Received 15 February 2007; in final form 31 May 2007)

The purpose of this paper is to investigate the effect of a twist on the losses of leaky modes in microstructured optical fibers (MOF). A helicoidal system of coordinates is introduced to define the structure and to set up the problem. These coordinates, albeit non-orthogonal, preserve the translational invariance in a way that allows a two-dimensional finite element model similar to that of classical straight waveguides. The Perfectly Matched Layer (PML) technique is used to compute the leaky modes in the fibers. Helicoidal coordinates and PML are unified under the point of view of geometrical transformations which allows the design of 'twisted PML' that provides the right tool to determine the leaky modes in the twisted structures.

1. Introduction

1.1 *Leaky modes in twisted microstructured fibers*

Microstructured optical fibers (MOF) became, in the last decade, an important device in classical optics. The classical model for such fibers is to consider a finite cladding of air holes in an infinite bulk of dielectric material, e.g. silica, with a central defect where the signal can propagate. In such a model, the refractive index at infinity is equal to the largest value of the refractive index in the whole fiber. In this case, it has been shown that there is no true mode propagating along the structure, i.e. corresponding to a real valued propagating constant and to electromagnetic fields of finite energy in the cross-section [1]. Nevertheless, there may be leaky modes corresponding to a complex valued propagating constant and to electromagnetic fields diverging exponentially at infinity in the cross-section. At first sight, such modes may seem useless but it appears that some configurations lead to a propagating constant with such an extremely small imaginary part that they are of practical interest. The numerical algorithms have therefore been extended to compute these leaky modes. In the finite element method, this is made via Perfectly Matched Layers (PML). The bare finite element method is unable to provide complex propagation constants because the propagation constants are computed as eigenvalues of Hermitian matrices and also because the corresponding fields are not in the suitable functional space. The introduction of the PML defines an extension of

*Corresponding author. E-mail: andre.nicolet@fresnel.fr

Waves in Random and Complex Media
ISSN: 1745-5030 (print), 1745-5049 (online)
http://www.tandf.co.uk/journals
DOI: 10.1080/17455030701481849

the involved operators such that the corresponding matrices are no longer Hermitian and that the corresponding diverging fields are damped to be included the finite element functional space [2].

Another problem is that during the production process of microstructured optical fibers, an uncontrolled twist may appear. The purpose of this paper is to determine the effect of this twist on the leaky modes. The modeling of ideal electromagnetic waveguides relies on their translational invariance to reduce the problem to a two-dimensional computation. In the case of twisted waveguides this invariance is lost. The proposed method presents a technique based on helicoidal coordinates to preserve the two-dimensional character of the computation of the modes (and/or the leaky modes) of such waveguides.

1.2 *Geometrical transformations in electromagnetism*

The basic principle of the methods presented in this paper is to transform a geometrical domain or a coordinate system into another one and to search how the equations to be solved have to be changed. As we start with a given set of equations in a given coordinate system, it seems at first sight that we have to map these coordinates on the new ones. Nevertheless it is the opposite that has to be done: the new coordinate system is mapped on the initial one (i.e. the new coordinates are defined as explicit functions of the initial coordinates) and the equations are then pulled back, according to differential geometry [3], on the new coordinates. This requires only the computation of the Jacobian (matrix) $\mathbf{J}$ made of the partial derivatives of the new coordinates with respect to the original ones.

In electromagnetism, such a change of coordinates amounts to replacing the different materials (often homogeneous and isotropic, which corresponds to the case of scalar piecewise constant permittivities and permeabilities) by equivalent inhomogeneous anisotropic materials described by a transformation matrix $\mathbf{T} = \mathbf{J}^T\mathbf{J}/det(\mathbf{J})$ [1, 4, 5].

From a geometric point of view, the matrix $\mathbf{T}$ is a representation of the metric tensor. The only thing to do in the transformed coordinates is to replace the materials (homogeneous and isotropic) by equivalent ones whose properties are given by the permittivity and permeability tensors:

$$\underline{\underline{\varepsilon}}' = \varepsilon\mathbf{T}^{-1}, \quad \text{and} \quad \underline{\underline{\mu}}' = \mu\mathbf{T}^{-1}. \tag{1}$$

We note that there is no change in the impedance of the media since the permittivity and permeability suffer the same transformation. As for the vector analysis operators and products, everything works as if we were in Cartesian coordinates.

In the more general case where the initial $\underline{\underline{\varepsilon}}$ and $\underline{\underline{\mu}}$ are tensors corresponding to anisotropic properties, the equivalent properties become

$$\underline{\underline{\varepsilon}}' = \mathbf{J}^{-1}\underline{\underline{\varepsilon}}\mathbf{J}^{-T}det(\mathbf{J}), \quad \text{and} \quad \underline{\underline{\mu}}' = \mathbf{J}^{-1}\underline{\underline{\mu}}\mathbf{J}^{-T}det(\mathbf{J})\,. \tag{2}$$

where $\mathbf{J}^{-1}$ is the inverse of the Jacobian matrix and $\mathbf{J}^{-T} \equiv (\mathbf{J}^{-1})^T$ the transpose of this inverse.

We will also need to consider compound transformations. Let us consider three coordinate systems $\{u, v, w\}$, $\{X, Y, Z\}$, and $\{x, y, z\}$. The two successive changes of coordinates are given by $\{X(u, v, w), Y(u, v, w), Z(u, v, w)\}$ and $\{x(X, Y, Z), y(X, Y, Z), z(X, Y, Z)\}$. They lead to the Jacobians $\mathbf{J}_{Xu}$ and $\mathbf{J}_{xX}$ so that

$$\mathbf{J}_{xu} = \mathbf{J}_{xX}\mathbf{J}_{Xu}. \tag{3}$$

This rule naturally applies for an arbitrary number of coordinate systems. The total transformation can therefore be considered either as involving a total Jacobian built according to equations (3), or as successive applications of equations (2). Note that the maps are defined

from the final $\{u, v, w\}$ to the original $\{x, y, z\}$ coordinate system and that the product of the Jacobians, corresponding to the composition of the pull back maps, is in the opposite order.

2. Helicoidal coordinates

Let us introduce a helicoidal coordinate system [6–8] (ξ_1, ξ_2, ξ_3) deduced from rectangular Cartesian coordinates (x, y, z) in the following way

$$\begin{cases} x = \xi_1 \cos(\alpha\xi_3) + \xi_2 \sin(\alpha\xi_3), \\ y = -\xi_1 \sin(\alpha\xi_3) + \xi_2 \cos(\alpha\xi_3), \\ z = \xi_3, \end{cases} \tag{4}$$

where α is a parameter which characterizes the torsion of the structure. A *twisted structure* is a structure for which both geometrical and physical characteristics (here the permittivity ε and the permeability μ) together with the boundary conditions only depend on ξ_1 and ξ_2. Note that such a structure is invariant along ξ_3 but $\frac{2\pi}{\alpha}$-periodic along z (the period may be shorter depending on the symmetry of the cross-section).

This general coordinate system is characterized by the Jacobian of the transformation (4):

$$\begin{aligned} \mathbf{J}_{\text{hel}}(\xi_1, \xi_2, \xi_3) &= \frac{\partial(x, y, z)}{\partial(\xi_1, \xi_2, \xi_3)} \\ &= \begin{pmatrix} \cos(\alpha\xi_3) & \sin(\alpha\xi_3) & \alpha\xi_2 \cos(\alpha\xi_3) - \alpha\xi_1 \sin(\alpha\xi_3) \\ -\sin(\alpha\xi_3) & \cos(\alpha\xi_3) & -\alpha\xi_1 \cos(\alpha\xi_3) - \alpha\xi_2 \sin(\alpha\xi_3) \\ 0 & 0 & 1 \end{pmatrix}, \end{aligned} \tag{5}$$

which does depend on the three variables ξ_1, ξ_2 and ξ_3. On the contrary, the transformation matrix $\mathbf{T}_{\text{hel}}$ [1]:

$$\mathbf{T}_{\text{hel}}(\xi_1, \xi_2) = \frac{\mathbf{J}_{\text{hel}}^T \mathbf{J}_{\text{hel}}}{det(\mathbf{J}_{\text{hel}})} = \begin{pmatrix} 1 & 0 & \alpha\xi_2 \\ 0 & 1 & -\alpha\xi_1 \\ \alpha\xi_2 & -\alpha\xi_1 & 1 + \alpha^2(\xi_1^2 + \xi_2^2) \end{pmatrix}, \tag{6}$$

which describes the change in the material properties, only depends on the first two variables ξ_1 and ξ_2. The inverse matrix is:

$$\mathbf{T}_{\text{hel}}^{-1}(\xi_1, \xi_2) = \begin{pmatrix} 1 + \alpha^2\xi_2^2 & -\alpha^2\xi_1\xi_2 & -\alpha\xi_2 \\ -\alpha^2\xi_1\xi_2 & 1 + \alpha^2\xi_1^2 & \alpha\xi_1 \\ -\alpha\xi_2 & \alpha\xi_1 & 1 \end{pmatrix}. \tag{7}$$

It is useful to understand the mechanism of this independence on ξ_3 and this will also be helpful in the setting of 'twisted PML'. For this purpose, the map to helicoidal coordinates is decomposed into several steps.

First, the classical switch from Cartesian coordinates (x, y, z) to polar coordinates (ρ, θ, z) is introduced via a map from ρ, θ to x, y:

$$\begin{cases} x(\rho, \theta) = \rho \cos\theta \\ y(\rho, \theta) = \rho \sin\theta. \end{cases} \tag{8}$$

The associated Jacobian is

$$\mathbf{J}_{x\rho}(\rho,\theta)=\frac{\partial(x,y,z)}{\partial(\rho,\theta,z)}=\begin{pmatrix}\cos\theta & -\rho\sin\theta & 0\\ \sin\theta & \rho\cos\theta & 0\\ 0 & 0 & 1\end{pmatrix}=\mathbf{R}(\theta)\mathbf{diag}(1,\rho,1). \tag{9}$$

with

$$\mathbf{R}(\theta)=\begin{pmatrix}\cos\theta & -\sin\theta & 0\\ \sin\theta & \cos\theta & 0\\ 0 & 0 & 1\end{pmatrix} \text{ and } \mathbf{diag}(1,\rho,1)=\begin{pmatrix}1 & 0 & 0\\ 0 & \rho & 0\\ 0 & 0 & 1\end{pmatrix}.$$

$\mathbf{R}(\theta)$ has the well known properties: $\mathbf{R}(\theta)^{-1}=\mathbf{R}(\theta)^T=\mathbf{R}(-\theta)$.

Furthermore, the inverse transformation is given by the map:

$$\begin{cases}\rho(x,y)=\sqrt{x^2+y^2}\\ \theta(x,y)=2\arctan\left(\dfrac{y}{x+\sqrt{x^2+y^2}}\right).\end{cases} \tag{10}$$

and is associated to the Jacobian:

$$\mathbf{J}_{\rho x}(x,y)=\mathbf{J}_{x\rho}^{-1}(\rho(x,y),\theta(x,y))=\mathbf{diag}\left(1,\frac{1}{\rho(x,y)},1\right)\mathbf{R}(-\theta(x,y)). \tag{11}$$

Consider now the following sequence of four coordinate systems:

- ξ_1,ξ_2,ξ_3: the twisted coordinates defined by equations (4);
- ρ,φ,ξ_3: the cylindrical representation of these twisted coordinates;
- ρ,θ,z: the classical cylindrical coordinates;
- x,y,z: the classical Cartesian rectangular system;

together with the three coordinate transformations linking a member of the sequence to the next one. The global transformation is the helicoidal to Cartesian map and the corresponding Jacobian is the product of the Jacobians associated to the elementary transformations that provides a factorization of the global Jacobian.

Note that the $z=\xi_3$ coordinate is invariant through all the coordinate changes and the axial distance $\rho=\sqrt{x^2+y^2}=\sqrt{\xi_1^2+\xi_2^2}$ is same in the two 'cylindrical' representations while the azimuthal angles are tied by a very simple relation

$$\theta=\varphi-\alpha z \tag{12}$$

simply indicating that the discrepancy between the two systems is a *local* rotation proportional to the position along z. The Jacobian of transformation (12) is:

$$\mathbf{J}_\alpha\equiv\mathbf{J}_{\theta\varphi}=\frac{\partial(\rho,\theta,z)}{\partial(\rho,\varphi,\xi_3)}=\begin{pmatrix}1 & 0 & 0\\ 0 & 1 & -\alpha\\ 0 & 0 & 1\end{pmatrix}.$$

The Jacobian of the Cartesian to helicoidal system is $\mathbf{J}_{\text{hel}}=\mathbf{J}_{x\rho}(\rho,\theta)\mathbf{J}_\alpha\mathbf{J}_{\rho x}(\rho,\varphi)$ and a direct computation gives:

$$\mathbf{J}_{\text{hel}}=\mathbf{R}(\theta)\underbrace{\begin{pmatrix}1 & 0 & 0\\ 0 & 1 & -\rho\alpha\\ 0 & 0 & 1\end{pmatrix}}_{\equiv\mathbf{J}_{\rho\alpha}}\mathbf{R}(-\varphi)=\begin{pmatrix}\cos(\alpha z) & \sin(\alpha z) & \alpha y\\ -\sin(\alpha z) & \cos(\alpha z) & -\alpha x\\ 0 & 0 & 1\end{pmatrix}. \tag{13}$$

The latest expression is obtained using the very definition of the cylindrical coordinates together with equations (12). Note that $det(\mathbf{J}_{\text{hel}}) = 1$.

An important fact is that $\mathbf{R}(\theta) = \mathbf{R}(\varphi)\mathbf{R}(-\alpha z)$ where $\mathbf{R}(-\alpha z)$ only depends on ξ_3 and $\mathbf{R}(\varphi)$ only depends on ξ_1 and ξ_2.

Introducing equations (13) in the definition of the $\mathbf{T}$ matrix, we have:

$$\mathbf{T}_{\text{hel}}(\xi_1, \xi_2) = \frac{\mathbf{J}_{\text{hel}}^T \mathbf{J}_{\text{hel}}}{det(\mathbf{J}_{\text{hel}})} = \mathbf{R}(\varphi)\mathbf{J}_{\rho\alpha}^T \mathbf{R}(-\theta)\mathbf{R}(\theta)\mathbf{J}_{\rho\alpha}\mathbf{R}(-\varphi)$$

$$= \mathbf{R}(\varphi)\begin{pmatrix} 1 & 0 & 0 \\ 0 & 1 & -\rho\alpha \\ 0 & -\rho\alpha & 1+\rho^2\alpha^2 \end{pmatrix}\mathbf{R}(-\varphi) = \begin{pmatrix} 1 & 0 & \alpha\rho\sin(\varphi) \\ 0 & 1 & -\alpha\rho\cos(\varphi) \\ \alpha\rho\sin(\varphi) & -\alpha\rho\cos(\varphi) & 1+\rho^2\alpha^2 \end{pmatrix}$$

and this latest expression is equal to the right hand member of equations (6). This computation shows clearly how the $\mathbf{R}(\theta)$ matrices cancel out to leave an expression that is an angle φ rotation of a matrix depending only on ρ, the axial distance, and therefore independent from the ξ_3 coordinate.

Note that $\mathbf{J}_{\text{hel}}|_{z=0} = \begin{pmatrix} \mathbf{I} & -\alpha\boldsymbol{\zeta} \\ 0 & 1 \end{pmatrix}$, with $\boldsymbol{\zeta} = \begin{pmatrix} -\xi_2 \\ \xi_1 \end{pmatrix}$ the $\pi/2$ counterclockwise rotation of $\boldsymbol{\xi}$, the position vector in the cross-section with respect to axis of rotation and $\mathbf{I}$ the 2×2 unit matrix. Since $\mathbf{T}_{\text{hel}}$ does not depend on $\xi_3 = z$, it can be computed from the Jacobian in any cross-section $\xi_3 = z =$ constant and therefore from $\mathbf{J}_{\text{hel}}|_{z=0}$. That provides a simple way to perform the computations together with a compact notation for the $\mathbf{T}_{\text{hel}}$ matrix and its inverse:

$$\mathbf{T}_{\text{hel}} = \begin{pmatrix} \mathbf{I} & -\alpha\boldsymbol{\zeta} \\ -\alpha\boldsymbol{\zeta}^T & 1+\alpha^2\boldsymbol{\zeta}^T\boldsymbol{\zeta} \end{pmatrix}, \mathbf{T}_{\text{hel}}^{-1} = \begin{pmatrix} \mathbf{I}+\alpha^2\boldsymbol{\zeta}\boldsymbol{\zeta}^T & \alpha\boldsymbol{\zeta} \\ \alpha\boldsymbol{\zeta}^T & 1 \end{pmatrix}. \tag{14}$$

3. Perfectly matched layers

3.1 *Classical cylindrical perfectly matched layers*

In the finite element analysis of wave problems in open space, one of the main difficulties is to truncate the unbounded domain. A common approach is to surround a finite region of interest with absorbing boundary conditions at finite distance. An alternative to conditions defined on the boundary is to introduce a special layer of finite thickness surrounding the region of interest such that it is non-reflecting and completely absorbing for the waves entering this layer under any incidence. Such regions have been introduced by Bérenger [9] and are called Perfectly Matched Layers (PML). Nowadays, the most natural way to introduce PML is to consider them as maps on a complex space [10, 11] so that the corresponding change of (complex) coordinates leads to equivalent ε and μ (that are complex, anisotropic, and inhomogeneous even if the original ones were real, isotropic, and homogeneous). This leads automatically to an equivalent medium with the same impedance as that of the initial ambient medium since ε and μ are transformed in the same way and this insures that the interface with the layer is non-reflecting. Moreover, a correct choice of the complex map leads to an absorbing medium able to dissipate the outgoing waves. The problem can therefore be properly truncated under the condition that the artificial boundary is situated in a region where the field is damped to a negligible value. To sum up, we have a problem in an unbounded region with outgoing propagating waves. A change of coordinates is performed such that it corresponds to the identity map in a region of interest (bounded, convex and, for all practical purposes,

with a simple shape) and to complex coordinates for the surrounding region. These complex coordinates are chosen to turn propagating waves to evanescent waves (i.e. exponentially decreasing at infinity) so that this outer domain can be truncated. As this new problem is related to the original one by a change of coordinates, it can be shown that the solution of the new problem matches perfectly the solution of the original problem in the region of interest where the map reduces to identity [2].

Given our helicoidal coordinate system, it is natural to introduce cylindrical PML. In this case, the PML corresponds to a complex stretch of the radial coordinate ρ, the *region of interest* is a disk defined by $\rho < R^*$, and the *PML region* is a circular annulus around the region of interest defined by $R^* < \rho < R^{\text{trunc}}$. R^* and R^{trunc} are real constants. As the expression of the material tensors in Cartesian coordinates are needed, the whole setting requires a transformation between Cartesian and cylindrical coordinates. The recipe involves a sequence of coordinate systems. We start here with the physical coordinates and we finish with the modelling coordinates. The mapping will therefore be from the last system of the list to the first one while the pull back maps will be from the first system to the last one.

- (x, y, z) are real valued classical Cartesian coordinates.
- $(\tilde{x}, \tilde{y}, \tilde{z})$ are a complex stretch of the previous Cartesian coordinates. They are complex valued and it is fundamental to understand that this change is an active transformation rather than a mere change of coordinates in the sense that the ambient space is changed. (x, y, z) are a parametrization of $\mathbb{R}^3$ and the complex stretch corresponds to an extension of the problem to $\mathbb{C}^3$ and more precisely to a three dimensional subspace Γ of $\mathbb{C}^3$ (in terms of real dimensions $\mathbb{C}^3$ is six dimensional and $\mathbb{R}^3$ and Γ are three dimensional) [10, 11]. The map from Γ to $\mathbb{R}^3$ is chosen in such way that the restriction of this map to the region of interest is the identity map. The solution of the original problem on $\mathbb{R}^3$ can be extended analytically to $\mathbb{C}^3$ and then restricted to Γ. If the complex stretch is correctly chosen, this 'complexified' solution on Γ is evanescent where the physical solution involves outgoing or even exponentially diverging waves.
- $(\tilde{\rho}, \tilde{\theta}, \tilde{z})$ is a cylindrical representation of $(\tilde{x}, \tilde{y}, \tilde{z})$.
- (ρ_c, θ_c, z_c) are *real valued* cylindrical coordinates on Γ. They are related to $(\tilde{\rho}, \tilde{\theta}, \tilde{z})$ via $\tilde{\theta} = \theta_c$, $\tilde{z} = z_c$, and a radial complex stretch

$$\tilde{\rho} = \int_0^{\rho_c} s_\rho(\rho')d\rho' \tag{15}$$

  where s_ρ is a *complex valued function* of a *real variable*, i.e. $s_\rho = 1$ in the central region of interest defined by $\rho_c < R^*$ (the complex stretch corresponds to an identity map in this region) and s_ρ has a complex value in the PML defined by $R^* < \rho < R^{\text{trunc}}$.
- (x_c, y_c, z_c) are the Cartesian representation of (ρ_c, θ_c, z_c) and are also *real valued* coordinates that will be called *modeling coordinates*. This is the modeling space where the numerical approximations are written, where the finite element mesh is defined, and where all the outgoing waves are turned to evanescent ones so that the computation domain can be truncated.

In the end, only the real valued coordinates x, y, z and x_c, y_c, z_c are involved but the complex map corresponds to a complex valued Jacobian. In the case of cylindrical coordinates, $\tilde{\rho}$ and ρ_c are just introduced to compute the radial stretch. Note also that $\theta_c = \tilde{\theta}$ and therefore will be simply denoted θ. The Cartesian to cylindrical coordinates transformation is just used to obtain the Cartesian expression of the corresponding metric tensor. The Jacobian associated to these changes of coordinates are: $\mathbf{J}_{\tilde{x}\tilde{\rho}} = \mathbf{J}_{x\rho}(\tilde{\rho}, \theta), \mathbf{J}_{\tilde{\rho}\rho_c} = \mathbf{diag}(\frac{\partial \tilde{\rho}}{\partial \rho_c}, 1, 1) = \mathbf{diag}(s_\rho(\rho_c), 1, 1)$, $\mathbf{J}_{\rho_c x_c} = \mathbf{J}_{\rho x}(\rho_c(x_c, y_c), \theta(x_c, y_c))$ (using the matrix valued functions defined in equations (9)

and equations (11)). The global Jacobian is the product of the individual Jacobians:

$$\mathbf{J}_{PML} = \mathbf{J}_{\tilde{x}\tilde{\rho}}\mathbf{J}_{\tilde{\rho}\rho_c}\mathbf{J}_{\rho_c x_c} = \mathbf{R}(\theta)\mathbf{diag}\left(s_\rho, \frac{\tilde{\rho}}{\rho_c}, 1\right)\mathbf{R}(-\theta). \tag{16}$$

Note that *we solve in fact numerically the extended problem obtained by the complex stretch (15) and defined on* Γ *that have the very remarkable property to coincide with our original problem in the region of interest*. In order to comply with traditional notation in the PML context and to avoid cumbersome notations, we drop the c subscript associated to the modeling coordinates that will subsequently be denoted as ρ and (x, y, z) without any ambiguity. For isotropic uniform media outside the region of interest, the cylindrical PML characteristics are obtained by multiplying ε and μ by the following complex matrix:

$$\begin{aligned}
\mathbf{T}_{PML}^{-1} &= \mathbf{J}_{PML}^{-1}\mathbf{J}_{PML}^{-T}\det(\mathbf{J}_{PML}) \\
&= \mathbf{R}(\theta)\mathbf{diag}\left(\frac{\tilde{\rho}}{s_\rho\rho}, \frac{s_\rho\rho}{\tilde{\rho}}, \frac{s_\rho\tilde{\rho}}{\rho}\right)\mathbf{R}(-\theta) \\
&= \begin{pmatrix}
\dfrac{\rho s_\rho \sin(\theta)^2}{\tilde{\rho}} + \dfrac{\tilde{\rho}\cos(\theta)^2}{\rho s_\rho} & \sin(\theta)\cos(\theta)\left(\dfrac{\tilde{\rho}}{\rho s_\rho} - \dfrac{\rho s_\rho}{\tilde{\rho}}\right) & 0 \\
\sin(\theta)\cos(\theta)\left(\dfrac{\tilde{\rho}}{\rho s_\rho} - \dfrac{\rho s_\rho}{\tilde{\rho}}\right) & \dfrac{\rho s_\rho \cos(\theta)^2}{\tilde{\rho}} + \dfrac{\tilde{\rho}\sin(\theta)^2}{\rho s_\rho} & 0 \\
0 & 0 & \dfrac{\tilde{\rho}s_\rho}{\rho}
\end{pmatrix}.
\end{aligned}$$

This latest expression is the metric tensor in Cartesian coordinates (x, y, z) for the cylindrical PML and θ, ρ, $\tilde{\rho}$, and $s_\rho(\rho)$ are explicit functions of the variables x and y. Another remarkable property of the PML is that they provide the correct extension to non-Hermitian operators (since $\mathbf{T}_{PML}$ is complex and symmetric) that allows the computation of the leaky modes and this may be obtained via a correct choice of the PML parameters, namely R^*, R^{trunc}, and $s_\rho(\rho)$. The method used to compute these parameters is accurately described in [2].

3.2 *Twisted PML*

The computation of leaky modes in twisted waveguides requires the set up of PML in helicoidal coordinates. The basic principle is to insert the complex stretch on cylindrical coordinates as an intermediary step before the transformation from the cylindrical to the rectangular representations of helicoidal coordinates. Mixing the notations used for PML and helicoidal coordinates, the Jacobian is: $\mathbf{J}_{\text{hPML}} = \mathbf{J}_{\tilde{x}\tilde{\rho}}(\tilde{\rho}, \tilde{\theta})\mathbf{J}_\alpha\mathbf{J}_{\tilde{\rho}\rho_c}\mathbf{J}_{\rho_c\xi_c}(\rho_c, \varphi_c)$. Here also the c subscript of the modelling coordinates is dropped, $\tilde{\theta}$ is denoted as θ, and the Jacobian is:

$$\begin{aligned}
\mathbf{J}_{\text{hPML}} &= \mathbf{R}(\theta)\mathbf{diag}(1, \tilde{\rho}, 1)\mathbf{J}_\alpha\mathbf{diag}(s_\rho, 1, 1)\mathbf{diag}(1, \rho^{-1}, 1)\mathbf{R}(-\varphi) \\
&= \mathbf{R}(\theta)\begin{pmatrix} s_\rho & 0 & 0 \\ 0 & \tilde{\rho}/\rho & -\tilde{\rho}\alpha \\ 0 & 0 & 1 \end{pmatrix}\mathbf{R}(-\varphi)
\end{aligned} \tag{17}$$

Finally, the θ dependence disappears again and the resulting $\mathbf{T}$ matrix only depends on the cross-section coordinates:

$$\mathbf{T}_{hPML} = \mathbf{R}(\varphi)\begin{pmatrix} \frac{\rho s_\rho}{\tilde{\rho}} & 0 & 0 \\ 0 & \frac{\tilde{\rho}}{\rho s_\rho} & -\alpha\frac{\tilde{\rho}}{s_\rho} \\ 0 & -\alpha\frac{\tilde{\rho}}{s_\rho} & \frac{\rho(1+\alpha^2\tilde{\rho}^2)}{\tilde{\rho}s_\rho} \end{pmatrix}\mathbf{R}(-\varphi) \tag{18}$$

The inverse matrix $\mathbf{T}^{-1}_{hPML}$ are given by:

$$T^{-1}_{\mathrm{hPML}} = \begin{pmatrix} \dfrac{\tilde\rho\cos^2(\varphi)}{\rho s_\rho} + \dfrac{\rho(1+\alpha^2\tilde\rho^2)s_\rho\sin^2(\varphi)}{\tilde\rho} & \dfrac{\sin(2\varphi)\left(\tilde\rho^2-\rho^2(1+\alpha^2\tilde\rho^2)s_\rho^2\right)}{2\rho\tilde\rho s_\rho} & -\alpha\tilde\rho s_\rho\sin(\varphi) \\ \dfrac{\sin(2\varphi)\left(\tilde\rho^2-\rho^2(1+\alpha^2\tilde\rho^2)s_\rho^2\right)}{2\rho\tilde\rho s_\rho} & \dfrac{\tilde\rho\sin^2(\varphi)}{\rho s_\rho} + \dfrac{\rho(1+\alpha^2\tilde\rho^2)s_\rho\cos^2(\varphi)}{\tilde\rho} & \alpha\cos(\varphi)\tilde\rho s_\rho \\ -\alpha\tilde\rho s_\rho\sin(\varphi) & \alpha\cos(\varphi)\tilde\rho s_\rho & \dfrac{\tilde\rho s_\rho}{\rho} \end{pmatrix} \tag{19}$$

This is the expression of the 'twisted cylindrical PML tensor' in 'helicoidal Cartesian modeling coordinates' ξ_1, ξ_2 and all the quantities involved in the previous expressions can be given as explicit functions of these two variables:

$$\varphi = 2\ \arctan\left(\frac{\xi_2}{\xi_1+\sqrt{\xi_1^2+\xi_2^2}}\right),\ \rho=\sqrt{\xi_1^2+\xi_2^2},\ s_\rho(\rho)=s_\rho\left(\sqrt{\xi_1^2+\xi_2^2}\right),$$

$$\text{and}\quad \tilde\rho = \int_0^{\sqrt{\xi_1^2+\xi_2^2}} s_\rho(\rho')d\rho'.$$

4. Finite element modeling of twisted waveguides

Our goal is to obtain numerically the propagation modes in an electromagnetic waveguide twisted along the ξ_3-axis – and therefore described by its cross-section in the $\xi_1\xi_2$-plane. We choose to formulate the problem in terms of the electric field $\mathcal{E}$ with homogeneous boundary conditions, i.e. for a guide with perfectly conducting metallic walls (homogeneous Dirichlet boundary conditions) in order to set up the finite element model [12–14]. Anyway, the PML will be used to model the open space and the resulting model must be indifferent to the actual conditions on the truncation boundary corresponding to the outer circle of radius R^{trunc} (see figure 1).

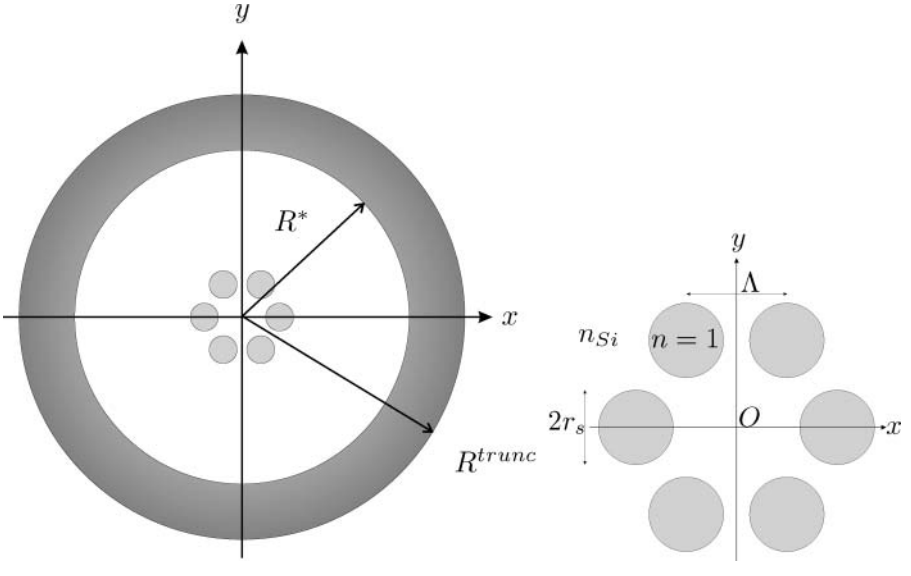

Figure 1. Cross-section of a twisted six hole MOF structure together with the surrounding annulus used to set up the PML ($R^* = 30\,\mu$m, $R^{\mathrm{trunc}} = 40\,\mu$m). On the right, a magnification of the hole structure with $\Lambda = 6.75\,\mu$m, $r_s = 2.5\,\mu$m, and $n_{\mathrm{Si}} = 1.444024$.

Choosing a time dependence in $e^{-i\omega t}$, and taking into account the invariance of the structure *in the local coordinates* (ξ_1, ξ_2, ξ_3) along the ξ_3-axis, we define the time-harmonic two-dimensional electric field $\mathbf{E}$:

$$\mathcal{E}(\xi_1, \xi_2, \xi_3, t) = \Re e(\mathbf{E}(\xi_1, \xi_2)\, e^{-i(\omega t - \beta \xi_3)}), \tag{20}$$

where $\omega = k_0 c = k_0/\sqrt{\mu_0 \varepsilon_0}$ is the angular frequency and β is the propagating constant of the guided mode. Note that $\mathbf{E}$ is a complex-valued field depending on two variables (coordinates ξ_1 and ξ_2) but still with three components (along the three axes). The two-dimensional electric field is separated into a transverse component $\mathbf{E}_t$ in the $\xi_1\xi_2$-plane and a longitudinal field E_ℓ along the ξ_3-axis (unit vector $\mathbf{e}^{\xi_3}$) of invariance so that $\mathbf{E} = \mathbf{E}_t + E_\ell \mathbf{e}^{\xi_3}$, with $\mathbf{E}_t \cdot \mathbf{e}^{\xi_3} = 0$. Note that the fact that the twisted coordinate system is not orthogonal leads not to any ambiguity about this scalar product since $\mathbf{e}^{\xi_3}$ is clearly always orthogonal to the $\xi_1\xi_2$-plane.

Writing Maxwell's equations in terms of $\mathbf{E}$, one gets

$$\mathbf{curl}_\beta \left(\mu_r^{-1}\, \mathbf{curl}_\beta\, \mathbf{E}\right) = k_0^2 \varepsilon_r \mathbf{E}, \tag{21}$$

where the operator $\mathbf{curl}_\beta$ is defined as $\mathbf{curl}_\beta\, \mathbf{U}(\xi_1, \xi_2) = \mathbf{curl}(\mathbf{U}(\xi_1, \xi_2) e^{i\beta\xi_3}) e^{-i\beta\xi_3}$ with $\mathbf{curl}$ having the same formal definition in terms of partial derivatives as in the case of rectangular Cartesian coordinates.

The discretization of Maxwell's equations (together with the equivalent material properties $\underline{\underline{\varepsilon_r}}'(\xi_1, \xi_2)$, $\underline{\underline{\mu_r}}'(\xi_1, \xi_2)$ corresponding to the twisted coordinates in the region of interest and to the twisted PML in the absorbing layer) is obtained via finite elements [1, 15]. The cross-section of the guide is meshed with triangles and Whitney finite elements are used, i.e. edge elements for the transverse field and nodal elements for the longitudinal field, to avoid spurious modes [1, 16].

Since the electric field satisfies a homogeneous Dirichlet boundary condition ($\mathbf{n} \times \mathbf{E} = 0$) on the boundary of the guide, the weak formulation of equations (21) writes

$$\mathcal{R}(\mathbf{E}, \mathbf{E}') = \int_\Omega \underline{\underline{\mu_r'}}^{-1}\, \mathbf{curl}_\beta\, \mathbf{E} \cdot \overline{\mathbf{curl}_{\bar\beta}\, \mathbf{E}'}\, d\xi_1 d\xi_2 - k_0^2 \int_\Omega \underline{\underline{\varepsilon_r'}} \mathbf{E} \cdot \overline{\mathbf{E}'}\, d\xi_1 d\xi_2 = 0,$$
$$\forall \mathbf{E}' \in H(\mathbf{curl}_\beta, \Omega), \tag{22}$$

where $\underline{\underline{\mu_r'}}^{-1} = \mu_r^{-1}\mathbf{T}$ and $\underline{\underline{\varepsilon_r'}} = \varepsilon_r \mathbf{T}^{-1}$ are the equivalent material properties. The μ_r and ε_r are the original material properties, that are isotropic and mostly piecewise homogeneous, and $\mathbf{T} = \mathbf{T}_{\text{hel}}$ in the region of interest disk and $\mathbf{T} = \mathbf{T}_{\text{hPML}}$ in the twisted PML annulus. The space $H(\mathbf{curl}_\beta, \Omega)$ of curl-conforming fields is defined as $H(\mathbf{curl}_\beta, \Omega) = \{\mathbf{v} \in [L^2(\Omega)]^3, \mathbf{curl}_\beta\, \mathbf{v} \in [L^2(\Omega)]^3\}$.

It is important to note that, even if $\overline{\beta}$ appears in equations (22), β^2 (and not $|\beta|^2 = \beta\overline{\beta}$) is involved in the complete development and, therefore, for fixed k_0, a generalized quadratic eigenvalue problem [17] is obtained for β. The involved matrices are not Hermitian since $\mathbf{T}_{\text{hPML}}$ is complex and symmetric and the computation of the eigenvalues provides the complex β corresponding to the leaky modes.

5. Numerical example

In order to check the model and to validate the choice of the parameters for the PML used in the numerical application, the value of the complex propagating constant in a waveguide that is not twisted is compared with the one obtained by using the multipole method. The philosophy of this latest method is completely different from those described in this paper and the reader can refer to [1] for a comprehensive review of this method. This method is

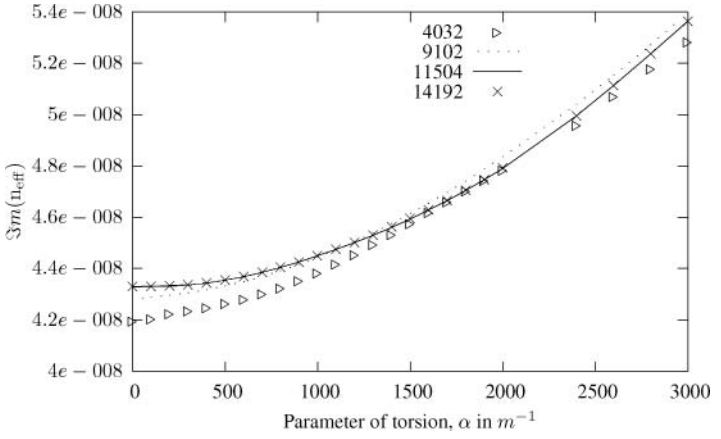

Figure 2. Imaginary part of the effective index $n_{\rm eff} = \beta/k_0$ for the fundamental mode versus the parameter of torsion α (m^{-1}) for various meshes. The results are good even for the coarser meshes ($\triangleright$ = 4032 elements and the dotted line = 9102 elements) and the discrepancy is unnoticeable between the curves for the finer meshes (the continuous line = 11504 elements and $\times$ = 14192 elements) indicating the mesh refinement in numerically convergent.

indeed well-suited for the step index MOF. We consider the hexagonal structure depicted in figure 1: this structure is a six hole MOF made up of a bulk of silica drilled by six air holes distant each other from $\Lambda = 6.75\,\mu$m. Each hole is circular with a radius equal to $r_s = 2.5\,\mu$m. A given wavelength $\lambda_0 = 1.55\,\mu$m is considered for which the index of silica is about $\sqrt{\varepsilon_{\rm Si}} = n_{\rm Si} = 1.444024$. Note that for this structure no propagating mode can be found and the fundamental mode is a leaky mode. The corresponding complex effective index, namely $n_{\rm eff} = \beta/k_0$ for the two different methods is $1.4387741 + 4.3257457\,10^{-8}i$ for the multipole method and $1.43877448 + 4.325885\,10^{-8}i$ for the finite element method. The practical implementation of the finite element model has been performed with COMSOL Multiphysics® software using a mesh of about 16,800 second order triangular elements and the computation takes about 150 seconds on a Pentium M 1.86 GHz, 1Go RAM laptop computer. Note that regarding its smallness with respect to the real part, the imaginary part is computed with an amazing accuracy: it is obtained with four figures though its value is smaller than the absolute error on the real part. The twisted problem is now considered to see how the fundamental leaky mode varies with respect to the torsion of the fiber. Still for the fundamental leaky mode and for a fixed k_0 corresponding to $\lambda_0 = 1.55\,\mu$m, two figures

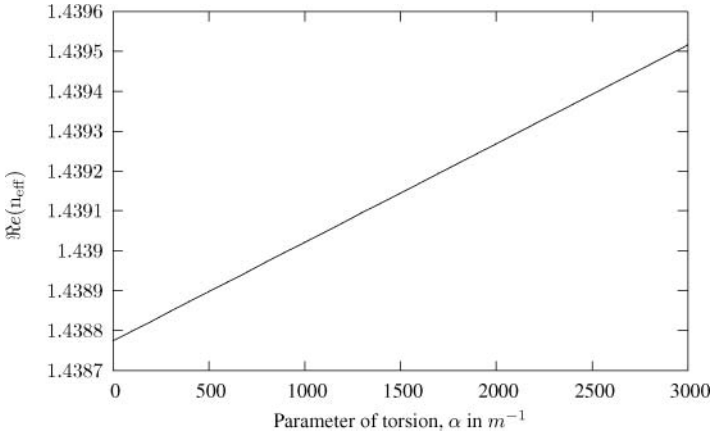

Figure 3. Real part of the effective index $n_{\rm eff} = \beta/k_0$ for the fundamental mode versus the parameter of torsion α (m^{-1}).

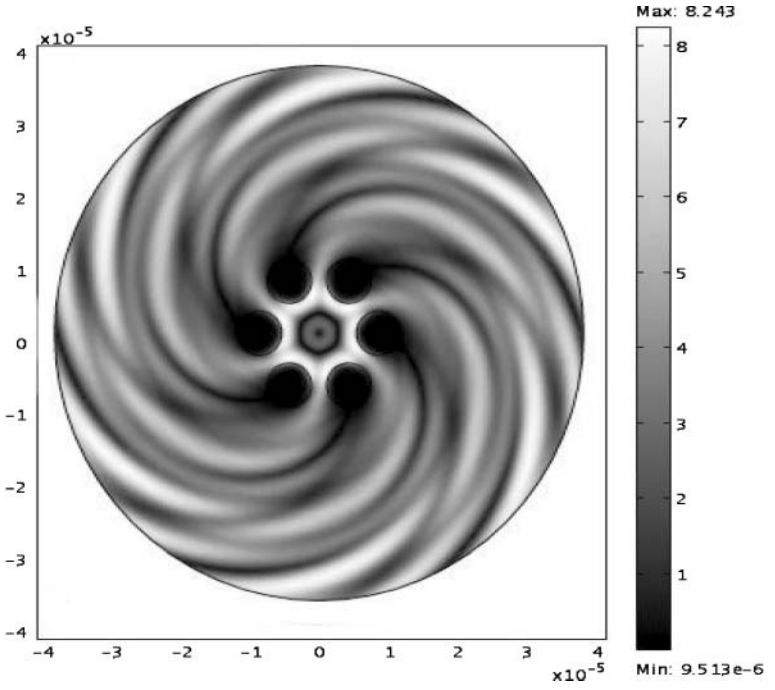

Figure 4. Map of the norm of the longitudinal component of the electric field $E_z = \alpha\xi_2 E_{\xi_1} - \alpha\xi_1 E_{\xi_2} + E_{\xi_3} = -\alpha\boldsymbol{\zeta}\cdot\mathbf{E}_t + E_\ell$ (see [15]) for a strongly twisted fiber ($\alpha = 50{,}000\,\mathrm{m}^{-1}$) with very large losses (see the last line of table 1). The map is truncated at the inner boundary of the PML, the field unit on the gray scale is arbitrary, and dimensions on the axes are in m.

are plotted representing $\Re e\{\beta/k_0\}$ (figure 3) and $\Im m\{\beta/k_0\}$ (figure 2) versus α, the parameter of torsion. It can be noticed that the relative influence of the torsion on the imaginary part is stronger than on the real part. The maximum torsion corresponds to $\alpha = 3000\,\mathrm{m}^{-1}$ so that the torsion length is $2\pi/\alpha = 2090\,\mu$m and taking into account the symmetry of the cross-section, the period of the torsion is in fact $\pi/3\alpha = 349\,\mu$m. This maximum torsion is weak with respect to the wavelength and the size of the cross-section pattern but strong with respect to the length of a real fiber. The perturbation of the fundamental mode with the increase of the losses does not seem to be strong enough to explain the poor quality associated to uncontrolled twist during the manufacturing process. Indeed this fundamental mode is remarkably stable with respect to a weak torsion and, for instance, the change of the imaginary part of the propagation constant by an order of magnitude requires a strong torsion (see table 1). Figure 4 shows the

Table 1. Evolution of the complex effective refractive index of the fundamental mode for large values of the parameter of torsion α. The computations have been performed with a fine 192256 element mesh.

$\alpha(\mathrm{m}^{-1})$	n_{eff}
0	$1.43877448428430 + 0.00000004326230i$
3000	$1.43803515386941 + 0.00000005379252i$
6000	$1.43729779697581 + 0.00000008159696i$
8000	$1.43680737693417 + 0.00000011432658i$
10000	$1.43631819034333 + 0.00000016617740i$
15000	$1.43822929902674 + 0.00000233000930i$
20000	$1.43541604442166 + 0.00002125238161i$
30000	$1.43134491668160 + 0.00004570591616i$
40000	$1.43145913422651 + 0.00010954672646i$
50000	$1.43464883801848 + 0.00097022365200i$

longitudinal electric field corresponding to the last line of this table where the large losses are associated to a non decreasing field.

6. Conclusion

In this paper, two techniques were simultaneously used to obtain the influence of a twist on the losses of leaky modes in microstructured optical fibers: the Perfectly Matched Layers which provide an extension of the operators that allows the finite element computation of the leaky modes together with the helicoidal system of coordinates that allows a two-dimensional approach to the computation of the propagating modes in twisted waveguides. The two techniques are unified in the framework of geometrical transformations and have been combined to provide 'twisted PML'. The versatility of the finite element method is necessary to cope with the anisotropy and inhomogeneity of the equivalent materials. A simple example is provided that demonstrates the effect of the twist on the leaky modes and specially on the imaginary part though this effect does not seem to be dramatic enough to jeopardize the behavior of weakly twisted fibers.

References

[1] Zolla, F., Renversez, G., Nicolet, A., Khulmey, B., Guenneau, S. and Felbacq, D., 2005, *Foundations of Photonic Crystal Fibres* (London: Imperial College Press).

[2] Ould Agha, Y., Zolla, F., Nicolet, A. and Guenneau, S., 2008, On the use of PML for the computation of leaky modes: an application to gradient index MOF. *The International Journal for Computation and Mathematics in Electrical and Electronic Engineering*, **27**. To appear.

[3] Bossavit, A., 1991, Notions de géométrie différentielle pour l'étude des courants de Foucault et des méthodes numériques en Électromagnétisme, *Méthodes numériques en électromagnétisme (A. Bossavit, C. Emson, I. Mayergoyz)*, Eyrolles, Paris, 1991, pp. 1–147, see also the English translation at http://www.lgep.supelec.fr/mse/perso/ab/DGSNME.pdf.

[4] Nicolet, A., Zolla, F. and Guenneau, S., 2004, Modelling of twisted optical waveguides with edge elements. *The European Physical Journal-Applied Physics*, **28**, 153–157, DOI: 10.1051/epjap:2004189.

[5] Nicolet, A., Movchan, A. B., Guenneau, S. and Zolla, F., 2006, Asymptotic modelling of weakly twisted electrostatic problems. *Comptes Rendus Mécanique*, **334**, 91–97.

[6] Lewin, L. and Ruehle, T., 1980, Propagation in twisted square waveguide. *Institute of Electrical and Electronics Engineers Transactions. Microwave Theory and Techniques*, **28**, 44–48.

[7] Yabe, H. and Mushiake, Y., 1984, An analysis of a hybrid-mode in a twisted rectangular waveguide. *Institute of Electrical and Electronics Engineers Transactions. Microwave Theory and Techniques*, **32**, 65–71.

[8] Igarashi, H. and Honma, T., 1991, A finite element analysis of TE modes in twisted waveguides. *Institute of Electrical and Electronics Engineers Transactions on Magnetics*, **27**, 4052–4055.

[9] Bérenger, J.-P., 1994, A perfectly matched layer for the absorption of electromagnetic waves. *Journal of Computational Physics*, **114**, 185–200.

[10] Lassas, M., Liukkonen, J. and Somersalo, E., 2001, Complex Riemannian metric and absorbing boundary condition. *Journal de Mathématiques Pures et Appliquées*, **80**, 739–768.

[11] Lassas, M. and Somersalo, E., 2001, Analysis of the PML equations in general convex geometry. *Proceedings of the Royal Society of Edinburgh, Section A: Mathematics*, **131**, 1183–1207.

[12] Guenneau, S., Nicolet, A., Zolla, F., Geuzaine, C. and Meys, B., 2001, A finite element formulation for spectral problems in optical fibers. *The International Journal for Computation and Mathematics in Electrical and Electronic Engineering*, **20**, 120–131.

[13] Guenneau, S., Nicolet, A., Zolla, F. and Lasquellec, S., 2002, Modeling of photonic crystal optical fibers with finite elements. *Institute of Electrical and Electronics Engineers Transactions on Magnetics*, **38**, 1261–1264.

[14] Guenneau, S., Lasquellec, S., Nicolet, A. and Zolla, F., 2002, Design of photonic band gap optical fibers using finite elements. *The International Journal for Computation and Mathematics in Electrical and Electronic Engineering*, **21**, 534–539.

[15] Nicolet, A. and Zolla, F., 2007, Finite element analysis of helicoidal waveguides. *Institution of Engineering and Technology Science, Measurement & Technology*, **1**, 67–70, DOI:10.1049/iet-smt:20060042.

[16] Bossavit, A., 1990, Solving Maxwell's equations in a closed cavity, and the question of spurious modes. *Institute of Electrical and Electronics Engineers Transactions on Magnetics*, **26**, 702–705.

[17] Tisseur, F. and Meerbergen, K., 2001, The quadratic eigenvalue problem. *Society for Industrial and Applied Mathematics Review*, **43**, 235–286.